

Optical solitons in a silicon waveguide

Jidong Zhang¹, Qiang Lin², Giovanni Piredda², Robert W. Boyd²,
Govind P. Agrawal², and Philippe M. Fauchet^{1,2}

¹Department of Electrical and Computer Engineering, University of Rochester, NY 14627

²The Institute of Optics, University of Rochester, Rochester, NY, 14627

jidong@ece.rochester.edu

Abstract: We observe, for the first time to our knowledge, the formation of optical solitons inside a short silicon waveguide (only 5 mm long) at sub-picojoule pulse energy levels. We measure a significant spectral narrowing in the anomalous-dispersion regime of such a waveguide, in contrast to all previous reported experiments. The extent of spectral narrowing depends on the carrier wavelength of input pulses, and the observed spectrum broadens in the normal-dispersion region. Numerical simulations confirm our experimental observations.

© 2007 Optical Society of America

OCIS codes: (190.4390) Nonlinear optics, integrated optics; (320.7130) Ultrafast processes in condensed matter, including semiconductors; (230.3990) Microstructure devices; (230.4000) Microstructure fabrication; (230.7370) Waveguides

References and links

1. R. Soref, "The Past, Present, and Future of Silicon Photonics," *IEEE J. Sel. Top. Quantum Electron.* **12**, 1678-1687 (2006).
2. V. R. Almeida, C. A. Barrios, R. R. Panepucci, and M. Lipson, "All-optical control of light on a silicon chip," *Nature* **431**, 1081-1084 (2004).
3. H. Rong, R. Jones, A. Liu, O. Cohen, D. Hak, A. Fang, and M. Paniccia, "A continuous-wave Raman silicon laser," *Nature* **433**, 725-728 (2005).
4. M. A. Foster, A. C. Turner, J. E. Sharping, B. S. Schmidt, M. Lipson, and A. L. Gaeta, "Broad-band optical parametric gain on a silicon photonic chip," *Nature* **441**, 960-963 (2006).
5. G. P. Agrawal, *Nonlinear Fiber Optics*, 4th ed. (Academic Press, Boston, 2007).
6. G. W. Rieger, K. S. Virk, and J. F. Young, "Nonlinear propagation of ultrafast 1.5 μm pulses in high-index-contrast silicon-on-insulator waveguides," *Appl. Phys. Lett.* **84**, 900-902 (2004).
7. O. Boyraz, T. Indukuri, and B. Jalali, "Self-phase-modulation induced spectral broadening in silicon waveguides," *Opt. Express* **12**, 829-834 (2004).
8. A. R. Cowan, G. W. Rieger, and J. F. Young, "Nonlinear transmission of 1.5 μm pulses through single-mode silicon-on-insulator waveguide structures," *Opt. Express* **12**, 1611-1621 (2004).
9. T. K. Liang, L. R. Nunes, T. Sakamoto, K. Sasagawa, T. Kawanishi, and M. Tsuchiya, "Ultrafast all-optical switching by cross-absorption modulation in silicon wire waveguides," *Opt. Express* **13**, 7298-7303 (2005).
10. R. Dekker, A. Driessen, T. Wahlbrink, C. Moormann, J. Niehusmann, and M. Först, "Ultrafast Kerr-induced all-optical wavelength conversion in silicon waveguides using 1.55 μm femtosecond pulses," *Opt. Express* **14**, 8336-8346 (2006).
11. E. Dulkeith, Y. A. Vlasov, X. Chen, N. C. Panoiu, and R. M. Osgood, Jr., "Self-phase-modulation in submicron silicon-on-insulator photonic wires," *Opt. Express* **14**, 5524-5534 (2006).
12. I. Hsieh, X. Chen, J. I. Dadap, N. C. Panoiu, R. M. Osgood, Jr., S. J. McNab, and Y. A. Vlasov, "Ultrafast-pulse self-phase modulation and third-order dispersion in Si photonic wire-waveguides," *Opt. Express* **14**, 12380-12387 (2006).
13. L. Yin, Q. Lin and G. P. Agrawal, "Dispersion tailoring and soliton propagation in silicon waveguides," *Opt. Lett.* **31**, 1295-1297 (2006).
14. L. Yin, Q. Lin and G. P. Agrawal, "Soliton fission and supercontinuum generation in silicon waveguides," *Opt. Lett.* **32**, 391-393 (2007).

15. H. K. Tsang, C. S. Wong, T. K. Liang, I. E. Day, S. W. Roberts, A. Harpin, J. Drake, and M. Asghari, "Optical dispersion, two-photon absorption and self-phase modulation in silicon waveguides at 1.5 μm wavelength," *Appl. Phys. Lett.* **80**, 416-418 (2002).
 16. Q. Lin, J. Zhang, P. M. Fauchet and G. P. Agrawal, "Ultrabroadband parametric generation and wavelength conversion in silicon waveguides," *Opt. Express* **14**, 4786-4799 (2006).
-

1. Introduction

Silicon photonics has attracted much attention recently because of its broad application potential from optical interconnects to biosensing [1]. In spite of its indirect band gap, silicon exhibits a significant third-order nonlinearity. This feature and a tight mode confinement provided by silicon-on-insulator (SOI) waveguides make it possible to realize a variety of optical functions at relatively low power levels on the chip level using CMOS-compatible fabrication technology [2]-[4].

One important nonlinear phenomenon is the formation of optical solitons. Solitons have been observed inside silica fibers, and they have found a multitude of applications ranging from optical switching to supercontinuum generation [5]. However, their formation generally requires a fairly long fiber because of silica's weak nonlinearity. In contrast, the nonlinear parameter γ in SOI waveguides can be larger by a factor of 10,000 or more. This feature makes it possible to form solitons within a very short length. Although significant efforts have been made to investigate pulse propagation in SOI waveguides [6]-[14], the formation of solitons has not been observed so far. In this paper, we demonstrate, for the first time to our knowledge, the formation of solitons inside a short SOI waveguide under appropriate device-design and pulse-launch conditions. In contrast to all other experiments where pulses experience spectral broadening, we observe a significant spectral narrowing and reshaping.

2. Waveguides design

Optical soliton results from a critical interplay between the effects of group-velocity dispersion (GVD) and self-phase modulation (SPM) [5]. The GVD-induced pulse broadening scales with the dispersion length $L_D = T_0^2/|\beta_2|$, where β_2 is the GVD coefficient and T_0 is the pulse width, whereas the SPM-induced chirp scales with the nonlinear length $L_n = (\gamma_0 P_0)^{-1}$, where $\gamma_0 = n_2 \omega_0 / (c a_{\text{eff}})$ is the nonlinear parameter and P_0 is the pulse peak power of pulses launched at the carrier frequency ω_0 into the fundamental waveguide mode with the effective mode area a_{eff} . The formation of a fundamental soliton requires $L_n = L_D \ll L$ for a waveguide of length L . Clearly, both $|\beta_2|$ and γ should be quite large for a soliton to be formed inside an SOI waveguide with $L < 1$ cm.

Fortunately, the tight mode confinement in SOI waveguides helps introduce significant waveguide dispersion and thus allows one to obtain a dramatically large anomalous GVD by designing the SOI waveguide appropriately. Figure 1 shows the calculated GVD curves for our waveguide. For dimensions of $860 \times 400 \text{ nm}^2$ and an etching depth of 300 nm (see the inset), the fundamental TM mode exhibits a GVD of $-2.26 \text{ ps}^2/\text{m}$ at 1500 nm. This value is more than 100 times larger than that of standard silica fibers ($< 0.02 \text{ ps}^2/\text{m}$). Even with such a high GVD, a dispersion length of ~ 1 mm still requires a pulse width of ~ 100 fs [13], a value much shorter than those used in most previous experiments [6]-[12]. In our experiments, we employ ultrashort pulses generated by an optical parametric amplifier (OPA). Our SOI waveguide has a zero-dispersion wavelength (ZDWL) near 1282 nm for the fundamental TM mode. Moreover, it has a small effective area of $a_{\text{eff}} = 0.13 \mu\text{m}^2$, which enhances the nonlinear parameter dramatically and thus enables a millimeter long nonlinear length with a fairly small input power.

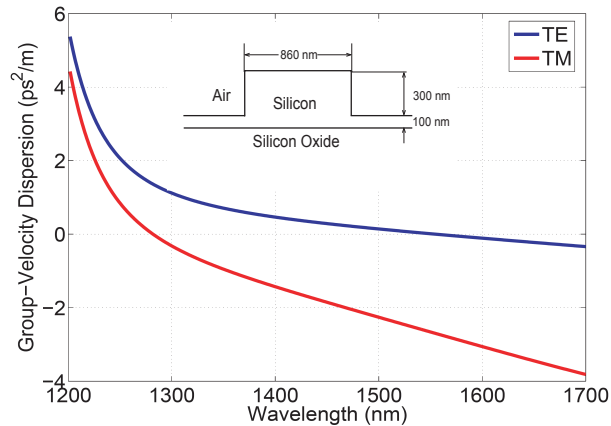


Fig. 1. Calculated dispersion curves for the TE and TM modes. The design of our waveguide is shown in the inset.

3. Experiments

Our waveguide is fabricated, using photolithography and reactive ion etching, along the $[1\ 1\ 0]$ direction on the $(1\ 0\ 0)$ silicon surface. It is tapered at both the input and output ends to enhance the coupling efficiency. The 5-mm-long waveguide has a propagation loss of about 5 dB/cm. Figure 2 shows our experimental setup. An OPA (Spectra Physics, OPA-800FC) provides nearly transform limited Gaussian pulses with a full width at half maximum (FWHM) of ~ 120 fs, at a repetition rate of 500 Hz. The carrier wavelength of the OPA output is tuned from 1.2 to 1.6 μm to cover both the normal and anomalous GVD regions of the waveguide. An achromatic objective lens couples the pulses into a single-mode fiber that delivers them to the waveguide. To reduce coupling losses, a lensed fiber taper (Nanonics Inc.) is used to couple the pulses into the waveguide. A second lensed fiber taper is used at the output end to efficiently deliver the pulses to an optical spectrum analyzer (OSA) (Ando AQ6315). The total coupling loss is estimated to be about 35 dB. The polarization state of the input pulses is adjusted by a polarization controller to align it along the TM mode. We maintain the input pulse energies within an appropriate range to prevent nonlinear effects inside the delivery fibers and to ensure that the pulses are affected by the nonlinear effects solely inside the SOI waveguide. This is verified by monitoring the spectrum of fiber output through an identical single-mode fiber with a length equal to the total length of the delivery fiber and the lensed fiber taper.

Figure 3 shows the input and output spectra at a carrier wavelength of 1484 nm in the deep anomalous-dispersion regime. The Gaussian input pulse spectrum shown on the top by a blue

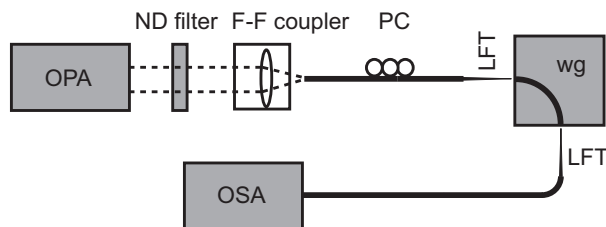


Fig. 2. Schematic of our experimental setup. F-F coupler: free-space-to-fiber coupler, PC: polarization controller, LFT: lensed fiber taper, WG: waveguide.

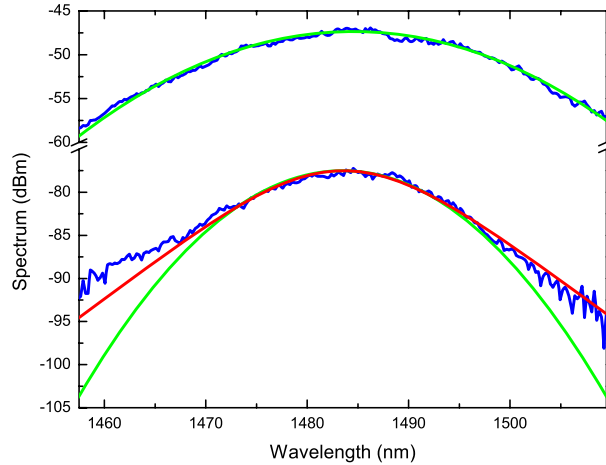


Fig. 3. Input (top) and output (bottom) pulse spectra measured at 1484 nm (blue curves) for an input pulse energy of 0.52 pJ. The green and red curves show the Gaussian and “sech” fits respectively to the data, as described in the text.

trace is parabolic on a semilog scale, and it is well fitted with a Gaussian function:

$$S_{\text{input}}(\lambda) = S_0 \exp \left[-\frac{(\lambda - \lambda_c)^2}{2\sigma^2} \right] \quad (1)$$

where λ_c is the center wavelength, S_0 is a constant factor and σ is the root-mean-square (rms) width. The fitted spectrum has a 3-dB bandwidth of 27.8 nm. As long as the input pulse energy remains low enough to avoid nonlinear effects inside the waveguide, the pulse spectrum does not change its shape. However, when the pulse energy increases beyond a certain value, the output spectrum begins to narrow down. The bottom blue trace in Fig. 3 shows the spectral narrowing at an input pulse energy of 0.52 pJ. This spectrum could not be fitted with the Gaussian function in Eq. (1), but agrees well with the hyperbolic secant shape associated with a soliton (red curve):

$$S_{\text{output}}(\lambda) = S_0 \text{sech}^2[(\lambda - \lambda_c)/\Delta\lambda] \quad (2)$$

where $\Delta\lambda$ is related to the FWHM by $\text{FWHM} = 2 \ln(1 + \sqrt{2})\Delta\lambda$. The 3-dB spectral bandwidth at this energy level is 18.8 nm, only about two thirds of the input one. This observation is in strong contrast to all other reported experiments, where spectral broadening was observed. Moreover, unlike the parabolic shape of the input spectrum, the output spectrum exhibits a nearly triangular shape on the semilog scale. These experimental results suggest strongly the formation of an optical soliton inside the SOI waveguide. Note that the required energy of input pulses here is more than two orders of magnitude smaller than that required in standard silica fibers, conforming the significant advantage of SOI waveguides for low-power nonlinear signal processing.

We have observed such a spectral narrowing over a broad wavelength range within the anomalous dispersion region, however less narrowing occurs as the carrier wavelength approaches the ZDWL. For example, the 3-dB output spectral bandwidth is 19 nm at 1350 nm, about 74% of the input value. At this wavelength, the output spectrum is neither Gaussian nor is described by a $\text{sech}^2(\omega)$ function, but a combination of the two. When the carrier wavelength is tuned toward 1249 nm into the normal dispersion regime (see Fig. 4), the output spectrum is broadened, not narrowed.

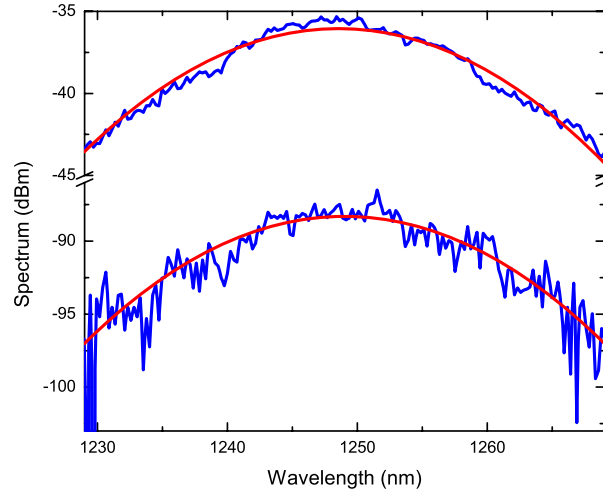


Fig. 4. Input (top) and output (bottom) pulse spectra measured at 1249 nm (blue curves). Red curves show a Gaussian fit to the experimental data.

4. Theory and simulations

Our experimental observations can be understood as follows. At the wavelength of 1484 nm, our waveguide has an anomalous GVD of $-2.15 \text{ ps}^2/\text{m}$. For a Gaussian pulse with a FWHM of 116 fs (corresponding to $T_0 = 70 \text{ fs}$), the dispersion length is only 2.28 mm. For an input pulse energy of 0.52 pJ, the nonlinear length at the input end is 1.23 mm, assuming $n_2 = 6 \times 10^{-5} \text{ cm}^2/\text{GW}$ [15]. Both are much shorter than the waveguide length. As a result, the interplay between SPM and GVD causes the pulses to evolve into a soliton. The soliton order [5] $N = (L_D/L_n)^{1/2} \approx 1.35$ exceeds 1 at the input end because a higher peak power is needed to compensate for TPA and linear scattering losses. Such a soliton corresponds to a path-averaged soliton [13]. When the pulse wavelength is tuned towards the ZDWL, the reduced GVD increases the dispersion length considerably. For example, GVD is only $-0.95 \text{ ps}^2/\text{m}$ at 1350 nm, leading to a dispersion length of 6 mm, larger than the waveguide length. Even though N is now larger, the pulse remains in the transition stage till the output end, resulting in a composite spectral shape in between a Gaussian and a function of $\text{sech}^2(\omega)$. In contrast, when the pulse wavelength is tuned to 1249 nm, GVD become positive ($0.81 \text{ ps}^2/\text{m}$). The SPM-induced chirp in this case accelerates GVD-induced pulse broadening, which in turn reduces the SPM effects. As a result, the output spectrum is broadened slightly.

To confirm our interpretation and to better understand the underlying physics, we have performed numerical simulations using the generalized nonlinear Schrödinger equation [5]:

$$\frac{\partial A}{\partial z} + \frac{1}{2}\alpha A - i \sum_{m=2}^8 \frac{i^m \beta_m}{m!} \frac{\partial^m A}{\partial \tau^m} = i\gamma|A|^2 A, \quad (3)$$

where β_m is the m th-order dispersion parameter at the carrier frequency ω_0 . The nonlinear parameter $\gamma = \gamma_0(1 + ir)$, where the dimensionless TPA parameter $r = c\beta_T/(2n_2\omega_0)$ includes TPA. For $n_2 = 6 \times 10^{-5} \text{ cm}^2/\text{GW}$ and $\beta_T = 0.45 \text{ cm}/\text{GW}$ [15], its value is close to 0.1. The loss factor $\alpha = \alpha_l + \alpha_f$ includes both the linear scattering loss α_l (assumed to be frequency independent) and time-dependent free-carrier absorption (FCA) $\alpha(z, \tau)$ [16]. Our simulations include the temporal dynamics of FCA but a detailed analysis shows that its effect is negligible for such short pulses at a relatively low repetition rate.

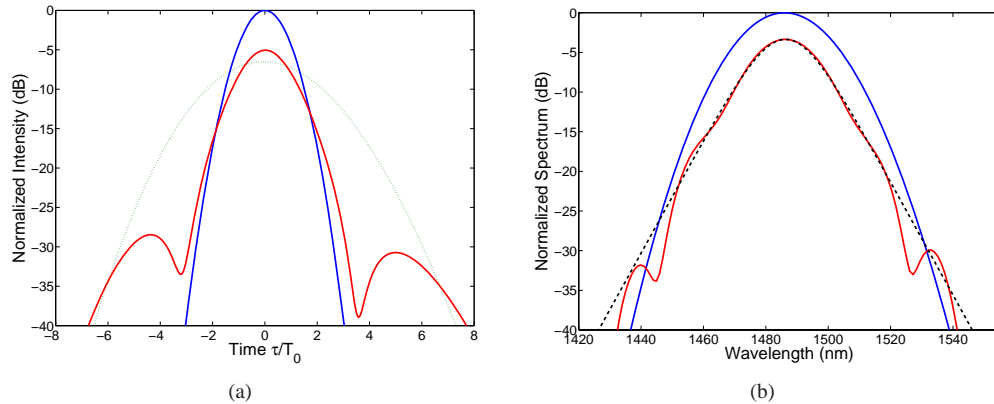


Fig. 5. Simulated temporal shape (a) and spectrum (b) of input (blue curves) and output (red curves) pulses under experimental conditions of Fig. 3. The dotted curve in (a) shows the output pulse with negligible nonlinear effects. The dashed curve in (b) corresponds to a sech pulse.

Figure 5 shows numerically simulated shapes and spectra of output pulses under our experimental conditions. At a very low power level for which the nonlinear effects are negligible (dashed curve), GVD broadens the pulse four-fold in the time domain, but its spectrum remains unchanged (except for a reduced magnitude because of linear losses). However, when input pulse energy increases to 0.52 pJ, the pulse is only slightly broadened in time (by about 18%) and adjusts its shape to evolve into a soliton. This can be seen more clearly in the spectral domain, where the output spectrum (red curve) is well described by a $S(\lambda)$ in Eq. (2) (dashed curve) at power levels up to -20 dB from the spectral peak. Moreover, the output spectrum is narrower by about 25%, which agrees well with our experimental observations, which is shown in Fig. 5(b).

To indicate how well our numerical simulations agree with the experiment, we compare the numerical output spectrum with the actual data in Fig. 6. It is important to stress that no fitting parameters were used in this comparison. It is very clear that experimental results agree well with numerical simulations. A slightly larger spectral narrowing in our experiment may be related to uncertainty in the experimental value of the pulse parameters. It may also have its origin in a small chirp on our input pulses. Numerical simulations were carried out assuming unchirped pulses.

5. Conclusions

In conclusion, we have observed the formation of optical solitons inside a short SOI waveguide (only 5 mm long). Our experimental conditions were such that both the dispersion and nonlinear lengths were considerably shorter than the device length, thus allowing soliton evolution over multiple soliton periods. We observed a significant spectral narrowing in the anomalous-dispersion regime, in contrast to all previous reported experiments. The extent of spectral narrowing depended on the carrier wavelength of input pulses because of changes in group-velocity dispersion. The numerical simulations confirm our experimental observations. Our demonstration should transfer many soliton-based signal processing techniques directly to silicon devices on the chip scale, especially because such a device requires relatively low pulse energies (<1 pJ).

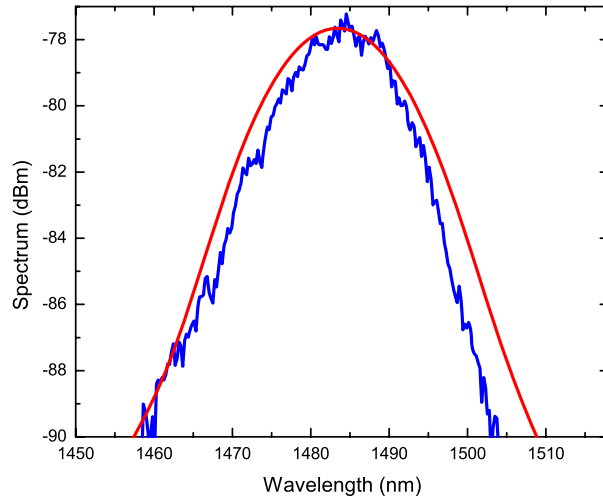


Fig. 6. Comparison between numerically simulated (red curve) and measured (blue curve) pulse spectra. Shape of the recorded spectrum agrees well with our numerical simulations. A slightly higher narrowing in the experimental is probably due to a small chirp on our input pulses.

Acknowledgements

The authors thank H. Shin for assistance with the laser system. This work was performed in part at the Cornell NanoScale Facility, a member of the National Nanotechnology Infrastructure Network, and we thank G. J. Bordonaro and M. Metzler for their advice on sample preparation. This work was supported in part by AFOSR and by Intel Corp.